Photoemission spectroscopy—Correspondence between quantum theory and experimental phenomenology*

Peter J. Feibelman†
Department of Physics, State University of New York, Stony Brook, New York 11790

D. E. Eastman
IBM Thomas J. Watson Research Center, Yorktown Heights, New York 10598
(Received 30 May 1974)

We describe the relation between the observed behavior of photoemission energy distributions vs frequency, angle, etc., and the quantum theory of photoemission as recently set forth formally by Caroli *et al*. We derive a Fermi's Golden-Rule formula for the angle- and energy-resolved photocurrent from an independent electron solid, and show in detail the approximations which render this formula equivalent to that of the familiar three-step model of bulk photoemission. In terms of the Golden-Rule formula, we account for the direct-transition band-structure regime generally observed at low photon energies ($h\nu \lesssim 20$–30 eV) and the "photoemission density of states", or x-ray-photoemission-spectroscopy regime, observed at higher energies. We also propose an explanation of Feuerbacher *et al.*'s observation of "direct photoemission into the vacuum" from single-crystal tungsten surfaces. Finally, we discuss the criteria which determine the relative magnitudes of photocurrents from a surface adsorbate layer and an underlying substrate.

I. INTRODUCTION

Photoemission is an experiment which is in principle rich in information; the independent parameters against which photocurrents can be measured include the frequency, polarization, and angle of incidence of the photons, the crystal face and surface structure of the target, and the energy, exit angle, and spin polarization of the electrons. Recently, there has been considerable interest in expanding one's knowledge of the behavior of photocurrents in this multidimensional space of parameters.[1–12]

As a result, one has observed several important trends which lend insight into the question of what photoemission measures. For example, consider the variation with photon frequency ν of angle-integrated photoemission energy distributions (PED's) from polycrystalline targets.[13] In many cases (see, e.g., Fig. 1 for Au) one sees the following: (a) At low frequencies (typically $h\nu \lesssim 20$ eV) there are many features in the PED's which change in position and shape as a function of ν. (b) At higher frequencies, features in the PED's are pretty much independent of $h\nu$, and seem to correspond to features in the target's occupied bulk density of states.

Also, there are sometimes peaks at low frequencies which do not move with ν but which can be identified with emission from "intrinsic," (i.e., clean-surface[9]) or "extrinsic" (i.e., adsorbate-induced) surface states.

Recent measurements of PED's versus electron exit angle have added at least one further possibility to this catalogue of PED peak behaviors. Feuerbacher *et al.*[9,14] have obtained PED's for electrons emerging along the normal to a W(110) surface, following excitation by photons with 7.7 eV $< h\nu <$ 11.7 eV. In this energy range, a band-structure calculation[14] indicates that there are no available Bloch states for the outgoing electron. At the same time, the measured PED's show a peak (at ~ 1.4 eV below E_F) which does not move with $h\nu$, and which is apparently not a surface peak. Feuerbacher and Christensen have identified this peak[14] with a peak in the W d-band density of states and have suggested, in view of the absence of an available outgoing Bloch state, that the electrons in this case have undergone "surface photoemission." We discuss this special case of "band-gap" photoemission below.

In general, in this article we hope to show how the qualitative description of PED's, given above, can be understood from the theoretical point of view. Our starting point is the recent work of Caroli *et al.*,[15] who have given an exact many-body formulation of photoemission including a recipe for the perturbative evaluation of the effects of electron-electron interaction to any order. In Sec. II we show how the lowest-order diagram of Caroli *et al.*,[13] which corresponds to photoemission from an independent- (but not necessarily "nearly-free-") electron solid, can be converted in general to a Fermi's Golden-Rule formula in which the final-state electron's wave function is identical to the wave function one would use to describe a low-energy-electron-diffraction (LEED) experiment with the incident LEED beam velocity $\vec{v}$ taken to equal minus the velocity of the photoelectrons being collected (see Fig. 2). This result, which was originally demonstrated by Adawi,[16] has been somewhat obscured in later theoretical work,[6,17] and, except

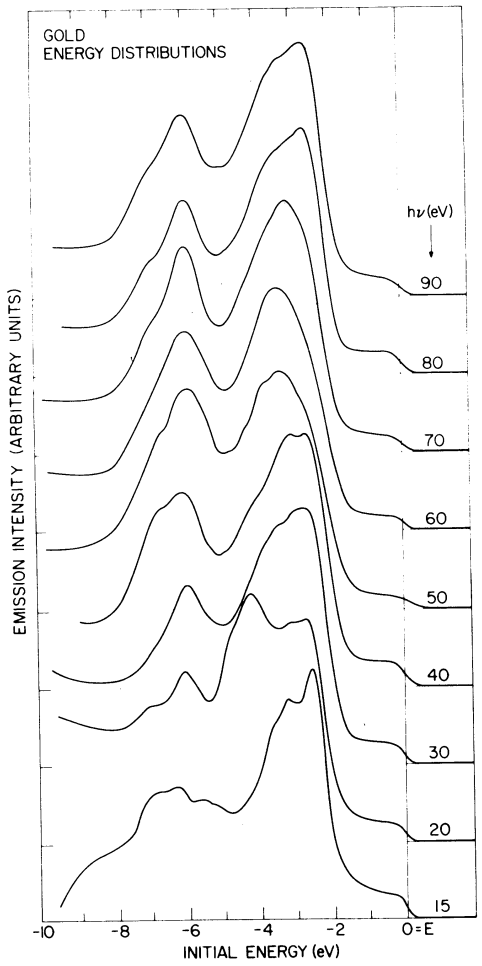

FIG. 1. Photoemission energy distributions (PED's) for Au as a function of photon frequency.[13] Notice the marked changes in peak shapes and positions with photon frequency in the lower frequency range ($h\nu \lesssim 30$ eV). These changes cease at higher frequencies, and the PED's then resemble the Au s- and d-band density of states.

for some efforts to identify the "surface photoeffect"[18] and to study photoemission from metals with adsorbate covered surfaces,[19] it has not been used in any attempt to analyze photoemission data quantitatively. (Such data are usually analyzed on the basis of the "three-step model" of bulk optical excitations followed by electron transport to, and escape through, the surface.)[20]

In Sec. III, we use the Golden-Rule formula, as modified to include electron mean-free-path effects, to develop a basis for understanding the behavior of photoemission spectra versus photon frequency. We focus on the effects of momentum conservation, and show for sufficiently weak electron damping that the Golden-Rule formula can be reduced to the semiclassical "three-step" model.[20] In this limit, the transition matrix elements for photoemission from the bulk become the usual crystal-momentum–conserving matrix elements which govern a solid's optical properties. Our derivation in Sec. III follows quite closely the procedure used by Mahan,[6] in deriving similar results for photoemission from a nearly-free-electron solid.

In Sec. IV, we use the Golden-Rule formula and develop criteria for when spectra show frequency-dependent structure due to momentum conservation (e.g., the "band-structure" regime) and for when the x-ray-photoemission-spectroscopy (XPS) regime (or weighted "density-of-states" regime[21]) occurs. We also discuss angle-resolved photoemission for the band-gap case and show that the surface contribution to the photocurrent can become significantly enhanced in favorable cases. Photoemission from localized adsorbate or adsorbate-induced "surface-molecule" states, is briefly described. For such states, relaxation effects usually preclude a direct photoemission measurement of the ground-state local density of states, although closely related spectral features can often be determined.

II. THEORY OF PHOTOEMISSION FROM AN INDEPENDENT-ELECTRON SOLID

A Fermi's Golden-Rule formula for photoemission from a solid was first derived in general by Adawi.[16] More recently, similar formulas have been derived by Mahan[6] and by Schaich and Ashcroft.[17] Mahan, in the context of what was the first theoretical description of the angular dependence of photoemission from a solid,[6] rederived the Golden-Rule formula for the special case in which the solid was assumed to be translationally invariant along the surface. Schaich and Ashcroft[17] also rederived this special case of Adawi's formula; they did so by way of illustrating their general, formal result, viz., that a photocurrent can be expressed exactly in terms of a three-current correlation function.

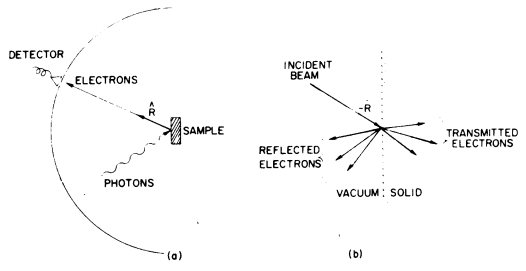

FIG. 2. (a) Schematic illustration of the arrangement of a photoemission experiment. The unit vector $\hat{R}$ points along the direction of the outgoing electrons. (b) Schematic illustration of the LEED experiment whose wave function enters the calculation of photocurrents. Note that the incident beam is directed at the sample along the direction $-\hat{R}$.

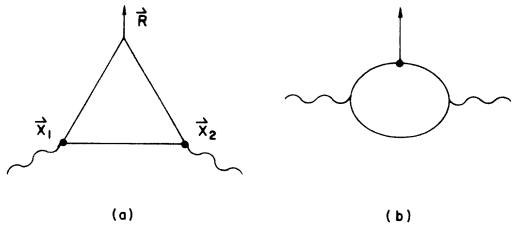

FIG. 3. (a) Lowest-order (independent-particle model) diagram for photoemission (after Ref. 15). The wavy lines represent photons, the heavy arrow represents the current of electrons at the detector. (b) Same diagram as in (a) drawn in such a way as to show that it represents a photoabsorption event in which a photoexcited electron is distinguished by being observed at a detector: If the arrow were removed from this diagram, it would look just like the lowest-order diagram for photoabsorption.

Although Mahan's and Schaich and Ashcroft's procedures for evaluating photocurrents from solids are in principle capable of accounting for many-body effects, it is only very recently that a straightforward perturbation theory of photoemission has been developed. Using the Keldysh perturbation theory[22] for nonequilibrium many-body problems, Caroli *et al.*[15] have set forth a formal diagrammatic expansion for photoemission from a solid. The lowest-order diagram (see Fig. 3) represents the photoemission process within the independent-electron picture. The higher-order terms describe many-body effects, such as the interaction of the photoelectron with the hole left behind, hole relaxation effects, the production of secondary electrons, etc.

In what follows, we focus exclusively on the lowest-order diagram. We show, independently of any assumption regarding the spatial form of the crystal potential,[23] that the algebraic expression to which this diagram corresponds can be reduced to the Fermi's Golden-Rule formula originally derived by Adawi.[16]

Thus, let us consider the irradiation of an independent-electron solid with light corresponding to the vector potential[24]

$$\vec{A}(\vec{x}, t) = \vec{A}(\vec{x}) \cos\omega t \,, \tag{1}$$

and the measurement [cf. Fig. 2(a)] of the steady radial current $j_r(\hat{R}, E)$ of electrons emerging from the solid along the observation direction, $\hat{R}$, with energies between E and $E+dE$.[25] For sufficiently low-intensity light, j_r is linear in the light intensity (quadratic in $\vec{A}$), and, using the method of Caroli *et al.*, can be shown[26] to be given by

$$j_r(\hat{R}; E) = \frac{1}{2\pi} \frac{e\hbar}{m} \left(\frac{e}{2mc}\right)^2 \lim_{\substack{\vec{R}'\to\vec{R} \\ \vec{R}\to\infty}} \left(\frac{\partial}{\partial R} - \frac{\partial}{\partial R'}\right)$$
$$\times \int\int d^3x_1 d^3x_2 \, G^r(\vec{R}, \vec{x}_1; E)$$
$$\times \hat{O}(\vec{x}_1) G^+(\vec{x}_1, \vec{x}_2; E - \hbar\omega) \hat{O}(\vec{x}_2) G^a(\vec{x}_2, \vec{R}'; E) \,. \tag{2}$$

In Eq. (2), the vector $\vec{R}$ is given by

$$\vec{R} = R\hat{R} \,, \tag{3}$$

where the unit vector $\hat{R}$ points in the direction of the detector. The operator $\hat{O}(x)$ is defined by

$$\hat{O}(\vec{x}) = \tfrac{1}{2}[\vec{A}(\vec{x}) \cdot \vec{p} + \vec{p} \cdot \vec{A}(\vec{x})] \,. \tag{4}$$

The functions $G^r(\vec{x}, \vec{x}'; E)$ and $G^a(\vec{x}, \vec{x}'; E)$, in Eq. (2), are, respectively, the ordinary retarded and advanced Green's functions for the solid, and $G^+(\vec{x}, \vec{x}'; E)$ is the nonlocal occupied density of states. The retarded Green's function satisfies the Dyson equation

$$G^r(\vec{x}, \vec{x}'; E) = G_0(\vec{x} - \vec{x}'; E) + \int d^3x_1 \, G_0(\vec{x} - \vec{x}_1; E) v(\vec{x}_1) G^r(\vec{x}_1, \vec{x}'; E) \,, \tag{5}$$

in which $v(\vec{x})$ is the crystal potential and $G_0(\vec{x} - \vec{x}'; E)$ is the free-particle outgoing-wave Green's function given by

$$G_0(\vec{x} - \vec{x}'; E) = \frac{m}{2\pi\hbar^2} \frac{\exp[i|\vec{x} - \vec{x}'|(2mE/\hbar^2)^{1/2}]}{|\vec{x} - \vec{x}'|} \,. \tag{6}$$

Both G^a and G^+ are functions which may be trivially evaluated once G^r is known. The advanced Green's function G^a is related to G^r by

$$G^a(\vec{x}, \vec{x}'; E) = [G^r(\vec{x}, \vec{x}'; E)]^* \,, \tag{7}$$

while the function G^+ is given by

$$G^+(\vec{x}, \vec{x}'; E) = -2i\Theta(-\Phi - E) \operatorname{Im} G^r(\vec{x}, \vec{x}'; E) \,, \tag{8}$$

where Φ is the solid's work function,[27] and $\Theta(x)$ is the ordinary step function. If the damping of holes is neglected, i.e., if the crystal potential is assumed to be real for energies below $-\Phi$, where the zero of energy is the vacuum level, then G^+ takes the form

$$G^+(\vec{x}, \vec{x}'; E) = 2\pi i \sum_{\text{occupied } j} \delta(E - E_j) \psi_j(\vec{x}) \psi_j^*(\vec{x}') \,, \tag{9}$$

where the sum on j includes all the occupied eigenstates of the Schrödinger equation

$$\left(-\frac{\hbar^2\nabla^2}{2m} + v(\vec{x}) - E_j\right) \psi_j(\vec{x}) = 0 \,. \tag{10}$$

This result, of course, follows directly from the spectral representation of G^r.

In order to put the expression for $j_r(\hat{R}; E)$, Eq. (2), into a useful form, one would like to be able

to evaluate the R and R' derivatives and the limits as $\vec{R}' \to \vec{R}$ and $R \to \infty$ explicitly, without first having to solve Eq. (5) for $G^r(\vec{x}, \vec{x}'; E)$. This goal, as was first pointed out by Adawi,[16] can be achieved because the asymptotic form of G^r, as $\vec{x}$ or $\vec{x}'$ is taken far outside the sample solid, can be exhibited in closed form.

One makes use of the fact that in the $\vec{x}_1$ integration of Eq. (5), the vector $\vec{x}_1$ is confined to the sample volume by the fact that $v(\vec{x}_1) = 0$ outside the sample.[28] Thus if $\vec{R}$ is a vector near the detector [cf. Fig. 2(a)], arbitrarily far from the sample, and if $\vec{x}'$ is a vector in the sample, then one has for *both* G_0's in Eq. (5) that

$$G_0(\vec{R} - \vec{x}; E) \approx \frac{m}{2\pi\hbar^2} \frac{\exp[i(2mE/\hbar^2)^{1/2}(R - \hat{R} \cdot \vec{x}' + \cdots)]}{R + \cdots} . \tag{11}$$

One thereby obtains the asymptotic formula for $G^r(\vec{R}, \vec{x}'; E)$,

$$G^r(\vec{R}, \vec{x}'; E) \underset{R \to \infty}{\longrightarrow} (m/2\pi\hbar^2)(e^{iR(2mE/\hbar^2)^{1/2}}/R) \times \phi_>(\vec{x}'; \hat{R}; E) , \tag{12}$$

where the wave function $\phi_>$ is given by

$$\phi_>(\vec{x}'; R; E) = e^{i\vec{k} \cdot \vec{x}'} + \int d^3x_1 \, e^{i\vec{k} \cdot \vec{x}_1} v(\vec{x}_1) G^r(\vec{x}_1, \vec{x}'; E) , \tag{13}$$

with

$$\vec{k} \equiv -(2mE/\hbar^2)^{1/2} \hat{R} . \tag{14}$$

The unit vector $\hat{R}$ points out of the sample at the detector (Fig. 2a). Therefore [cf. Fig. 2(b)] the wave vector $\vec{k}$ points into the sample along the direction of observation.

Using Eq. (12), as well as the symmetry relation

$$G^r(\vec{x}, \vec{x}'; E) = G^r(\vec{x}', \vec{x}; E) , \tag{15}$$

one may straightforwardly evaluate the R derivatives and the limits in Eq. (2). One finds that

$$\begin{aligned} R^2 j_r(\hat{R}; E) = 2ev \left(\frac{e}{2mc}\right)^2 \left(\frac{m}{2\pi\hbar^2}\right)^2 \\ \times \int d^3x_1 \, d^3x_2 \, \phi_>^*(\vec{x}_1; \hat{R}; E) \\ \times \hat{O}(\vec{x}_1) \frac{1}{2\pi i} G^+(\vec{x}_1, \vec{x}_2; E - \hbar\omega) \\ \times \hat{O}(\vec{x}_2) \phi_>(\vec{x}_2; \hat{R}; E) , \end{aligned} \tag{16}$$

or using Eq. (9), for the case in which hole damping may be neglected,

$$\begin{aligned} R^2 j_r(\hat{R}; E) = 2ev \left(\frac{e}{2mc}\right)^2 \left(\frac{m}{2\pi\hbar^2}\right)^2 \\ \times \sum_{\text{occupied } j} \delta(E - \hbar\omega - E_j) \\ \times \left| \int d^3x \, \phi_>^*(\vec{x}; \hat{R}; E) \hat{O}(\vec{x}) \psi_j(\vec{x}) \right|^2 . \end{aligned} \tag{17}$$

In Eqs. (16) and (17) the quantity v is the outgoing-electron velocity, equal to $(2E/m)^{1/2}$; the over-all factor 2 in these equations arises from spin summation.

Equation (17), which is identical in content to Adawi's Eq. (2.13b),[29] provides us with a useful recipe for calculating a photocurrent via a Fermi's Golden-Rule formula.[30] Specifically, it tells us that in the matrix elements governing the intensity of photoemission, the final electron state must be represented by the "incoming" wave function,[31] $\phi_>(\vec{x}; \hat{R}; E)$. This wave function is, in fact, identical to the wave function one would use to describe a LEED experiment in which electrons of energy E impinge on the sample along the direction $-\hat{R}$, a result which we now demonstrate.

Note first that asymptotically as $|\vec{x}'| \to \infty$, according to Eq. (13), $\phi_>(\vec{x}'; \hat{R}; E)$ is a linear combination of $e^{i\vec{k} \cdot \vec{x}'}$ and outgoing waves [$G^r(\vec{x}_1, \vec{x}'; E)$ being purely outgoing as $|\vec{x}'| \to \infty$]. Moreover, $\phi_>$ satisfies the Schrödinger equation

$$\left(-\frac{\hbar^2\nabla^2}{2m} + v(\vec{x}) - E\right) \phi_>(\vec{x}; \hat{R}; E) = 0 , \tag{18}$$

as can be seen from the symmetry relation, Eq. (15), together with the fact that

$$\left(E + \frac{\hbar^2\nabla^2}{2m} - v(\vec{x})\right) G^r(\vec{x}, \vec{x}'; E) = \delta(\vec{x} - \vec{x}') , \tag{19}$$

which follows from Eqs. (5) and (6). Thus $\phi_>$ satisfies both the correct equation of motion and the correct boundary conditions to be a LEED wave function, which was to be proven. Of course in photoemission, as Mahan has pointed out,[6] it is the components of $\phi_>$ which are transmitted into the solid that determine the observed results (since the $\psi_j(\vec{x})$'s fall rapidly to zero outside the sample), while in LEED it is, rather, the reflected components that represent what is measured.

Notice that in deriving Eq. (17) for the photocurrent, no specific spatial dependence of $v(\vec{x})$ had to be assumed. In particular, the assumption that $v(\vec{x}) = v(z)$, which Mahan used in proving the formula analogous to Eq. (17) for a free-electron solid, has been entirely avoided and therefore Eq. (17) is valid for the general case in which the lattice periodicity of $v(\vec{x})$ cannot be neglected.

Indeed, let us assume that the target under consideration is a semi-infinite crystal with an ideal (i.e., two-dimensionally periodic) surface. In this case, the wave functions $\phi_>$ and ψ_j behave as Bloch functions of the coordinates x and y along the surface, and the matrix elements in Eq. (17) there-

fore contain two-dimensional-crystal-momentum-conserving δ functions. This fact permits us to reduce Eq. (17) to a useful, more explicit form. The remainder of this section is devoted to that reduction.

Assuming then that our target has two-dimensional lattice periodicity, the wave function $\phi_>$ may be written in the form

$$\phi_>(\vec{x};\hat{R};E) = e^{i\vec{k}_{\parallel}^{(r)}\cdot\vec{\rho}}\, U(\vec{\rho},z;\hat{R};E)\ . \tag{20}$$

In Eq. (20), $\vec{\rho}\equiv(x,y)$, and $U(\vec{\rho},z;\hat{R},E)$ is periodic as a function of $\vec{\rho}$, with the two-dimensional periodicity of the target surface; i.e., for any $\vec{\rho}$, and for an arbitrary two-dimensional-lattice translation vector $\vec{\tau}$, one has

$$U(\vec{\rho},z;\hat{R};E) = U(\vec{\rho}+\vec{\tau},z;\hat{R};E)\ . \tag{21}$$

The vector $\vec{k}_{\parallel}^{(r)}$, in Eq. (20), is defined as follows: Let $\vec{k}_{\parallel}$ equal the projection of $\vec{k}$ [cf. Eq. (14)] in the plane of the surface. Then $\vec{k}_{\parallel}^{(r)}$ is the vector obtained by translating $\vec{k}_{\parallel}$ to the first two-dimensional Brillouin zone.[32]

In a similar fashion, the wave function $\psi_j(\vec{x})$ may be written

$$\psi_j(\vec{x}) \to \psi^{(n)}_{\vec{p}_{\parallel},p_n}(\vec{x}) = e^{i\vec{p}_{\parallel}\cdot\vec{\rho}}\, V^{(n)}_{\vec{p}_{\parallel},p_n}(\vec{\rho},z)\ , \tag{22}$$

where $V^{(n)}_{\vec{p}_{\parallel},p_n}(\vec{\rho},z)$ is a function having the periodicity of the target surface,[33] and where, in the reduced zone scheme, the implicit index j is replaced by $\vec{p}_{\parallel}$, a wave vector in the first two-dimensional Brillouin zone, n, a three-dimensional band index, and p_n, a wave vector normal to the surface.[34]

In order to complete our reduction of Eq. (17) it remains for us to describe the spatial behavior of the vector potential, $\vec{A}(\vec{x})$. Within the context of a calculation of photoemission based entirely on the diagram of Fig. 1, the variation of $\vec{A}(\vec{x})$ with $\vec{x}$ is the same inside the target as outside. This feature of the single diagram calculation is in error, especially at lower frequencies ($\lesssim 20$ eV); that is, a theory which failed to take account of the dielectric response of the target would in many instances be manifestly incapable of predicting photoyields, because the dielectric response can cause a substantial (polarization dependent) fraction of the incident photons to be reflected. Thus in order to be able to discuss photoemission for the entire range of frequencies, $\Phi < \hbar\omega \lesssim 500$ eV, one must supplement the diagram of Fig. 3 by those diagrams (shown in Fig. 4) which account for the screening of the incident electromagnetic field.

The net effect of including these additional diagrams is to replace the operator $\hat{O}(\vec{x})$, which appears in Eqs. (16) and (17), by the operator $\hat{O}_{sc}(\vec{x})$,

$$\hat{O}_{sc}(\vec{x}) = \tfrac{1}{2}[\vec{A}_{sc}(\vec{x})\cdot\vec{p} + \vec{p}\cdot\vec{A}_{sc}(\vec{x})]\ , \tag{23}$$

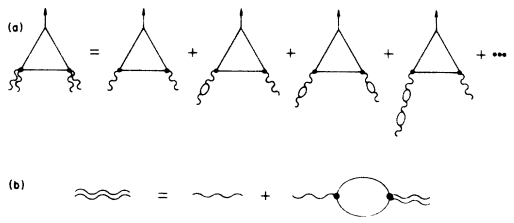

FIG. 4. (a) Diagram in which reflection and refraction of the photon beam by the sample has been taken into account. (b) Random-phase-approximation equation for the "dressed" photon propagator (represented by a double wavy line).

where, in the simplest microscopic approximation (illustrated in Fig. 4), the difference between the screened vector potential $\vec{A}_{sc}(x)$ and the externally applied $\vec{A}(x)$ is accounted for in terms of the solid's random-phase-approximation (RPA) dielectric tensor. Even in this simple approximation, however, it is not trivial to solve for $\vec{A}_{sc}(\vec{x})$, and therefore, rather than attempting to solve for it, one generally replaces the microscopic $\vec{A}_{sc}(\vec{x})$, in photoemission[35] calculations, by the macroscopic, Maxwell-equation-based approximation to it. That is, one imagines the exact screened vector potential to take the form

$$\vec{A}_{sc}(\vec{x}) = \hat{\epsilon}\,a(\vec{x}) + \delta\vec{A}(\vec{x})\ , \tag{24}$$

where $\hat{\epsilon}$ and $a(\vec{x})$ are, respectively, the polarization vector and the magnitude of the Maxwell-equation screened vector potential inside the target, and $\delta\vec{A}(\vec{x})$ is a "local-field" correction to $\hat{\epsilon}\,a(\vec{x})$ whose effects may be ignored to a first approximation.

This neglect of $\delta\vec{A}(\vec{x})$ is evidently exact only in the limit that the target is spatially homogeneous, or in other words, in the limit that it is an infinite (i.e., surfaceless), free-electron solid. Thus, any contribution to $\delta\vec{A}(\vec{x})$ for an actual target may be attributed either: (a) to the lattice periodicity of the target's charge density, or (b) to the presence of a surface. Local-field effects due to lattice periodicity are thought to be small for a wide class of materials.[36] Those due to the surface, which are conveniently thought of as refraction and reflection effects, have been studied theoretically within a number of simple models.[37] However, little is known about them experimentally. Clearly, if one wishes to use photoemission as a probe of surface chemistry, one will have to make a serious effort to evaluate surface-local-field effects.[18] In what follows, however, as in previous work, we ignore $\delta\vec{A}(\vec{x})$ entirely.

Let us assume, for simplicity, that $\hbar\omega \lesssim 200$ eV. Then the spatial dependence of $a(\vec{x})$ can be neglected, and we obtain the expression

$$\hat{O}_{sc}(\vec{x}) \approx -i\hbar a\hat{\epsilon}\cdot\nabla \tag{25}$$

where a is the spatially constant magnitude of the screened vector potential inside the target. The photoexcitation matrix element

$$\int d^3x\,\phi_f^*(\vec{x};\hat{R};E)\hat{O}_{sc}(\vec{x})\psi_j(\vec{x}) \tag{26}$$

therefore reduces to the form

$$(2\pi)^2\delta^{(2)}(\vec{k}_{\parallel}^{(r)}-\vec{p}_{\parallel})\int_{\Omega_2}d^2\rho\int dz\,U^*(\vec{\rho},z;\hat{R};E)\hbar a \times\left(\vec{\epsilon}_{\parallel}\cdot\vec{k}_{\parallel}^{(r)}+\frac{1}{i}\hat{\epsilon}\cdot\vec{\nabla}\right)V^{(n)}_{\vec{p}_{\parallel},p_n}(\vec{\rho},z)\,, \tag{27}$$

where $\vec{\epsilon}_{\parallel}$ is the projection of $\hat{\epsilon}$ in the plane of the surface, and where the $\vec{\rho}$ integration is over the volume, Ω_2, of the surface two-dimensional unit cell.[38] Substituting this result into Eq. (17) and, in the usual manner, interpreting $[(2\pi)^2\delta^{(2)}(\vec{k}_{\parallel}^{(r)}-\vec{p}_{\parallel})]^2$ as the target surface area S times $(2\pi)^2\delta^{(2)}\times(\vec{k}_{\parallel}^{(r)}-\vec{p}_{\parallel})$, one finds finally that

$$R^2j_r(\hat{R};E)=2e\mathfrak{F}S\,\frac{\alpha a_B}{\pi|\vec{\epsilon}_{\parallel}|}\,\frac{(\Re E)^{1/2}}{(\hbar\omega)^2} \times\sum_{n,p_n}\delta(E-\hbar\omega-E^{(n)}_{\vec{k}_{\parallel}^{(r)},p_n}) \times\left|\int_{\Omega_2}d^2\rho\int dz\,U^*(\rho,z;\hat{R};E) \times\left(\vec{\epsilon}_{\parallel}\cdot\vec{k}_{\parallel}^{(r)}+\frac{1}{i}\hat{\epsilon}\cdot\vec{\nabla}\right)V^{(n)}_{\vec{k}_{\parallel}^{(r)},p_n}(\vec{\rho},z)\right|^2. \tag{28}$$

In Eq. (28), the quantities α, a_B, $\Re$, and $\mathfrak{F}$ are, respectively, the fine-structure constant, the Bohr radius, the Rydberg, and the flux of electromagnetic energy per unit area per unit time, inside the target.[39] The latter is given by the expression

$$\mathfrak{F}\equiv\omega^2a^2|\vec{\epsilon}_{\parallel}|/8\pi c\,, \tag{29}$$

and is equal to the incident flux times one minus the target's reflectivity. The quantity $|\hat{\epsilon}_{\parallel}|$ is, of course, equal to the cosine of the angle of refraction of the photons.

One final reduction of our expression for $j_r(\hat{R};E)$ can be made by expressing the functions $V(\vec{\rho},z;\hat{R},E)$ and $V^{(n)}_{\vec{p}_{\parallel},p_n}(\vec{\rho},z)$ in the two-dimensional plane-wave representation. That is, the periodicity of these functions with $\vec{\rho}$ permits us to write

$$U(\vec{\rho},z;\hat{R};E)=\sum_{\vec{g}_{\parallel}}e^{i\vec{g}_{\parallel}\cdot\vec{\rho}}u_{\vec{g}_{\parallel}}(z;\hat{R};E) \tag{30}$$

and

$$V^{(n)}_{\vec{p}_{\parallel},p_n}(\vec{\rho},z)=\sum_{\vec{g}_{\parallel}}e^{i\vec{g}_{\parallel}\cdot\vec{\rho}}v^{(n)}_{\vec{g}_{\parallel},\vec{p}_{\parallel},p_n}(z)\,, \tag{31}$$

where the $\vec{g}_{\parallel}$ are two-dimensional reciprocal-lattice vectors. Substituting these expansion formulas into Eq. (28), one obtains the somewhat simpler expression for $j_r(\hat{R};E)$,

$$R^2j_r(\hat{R};E)=2e\mathfrak{F}S\,\frac{\alpha a_B}{\pi|\vec{\epsilon}_{\parallel}|}\,\frac{(\Re E)^{1/2}}{(\hbar\omega)^2} \times\sum_{\substack{n,p_n\\ \text{occupied}}}\delta(E-\hbar\omega-E^{(n)}_{\vec{k}_{\parallel}^{(r)},p_n}) \times\left|\sum_{\vec{g}_{\parallel}}\int dz\,u^*_{\vec{g}_{\parallel}}(z;\hat{R};E) \times\left(\vec{\epsilon}_{\parallel}\cdot(\vec{k}_{\parallel}^{(r)}+\vec{g}_{\parallel})+\frac{1}{i}\epsilon_{\perp}\frac{\partial}{\partial z}\right)v^{(n)}_{\vec{k}_{\parallel}^{(r)},p_n,\vec{g}_{\parallel}}(z)\right|^2, \tag{32}$$

in which $\epsilon_{\perp}$ is the component of $\hat{\epsilon}$ along the normal to the surface.

Note, in conclusion, that Eq. (28) [or equally, Eq. (32)] answers the often posed question of how photoemission data, taken by detecting electrons that are excited near a sample's surface [i.e., within an inelastic mean free path of it], can supply information regarding the sample's bulk density of states. The point is that, except for surface state energies, the $E^{(n)}_{\vec{k}_{\parallel}^{(r)},p_n}$ which appear in Eq. (28) for a semi-infinite sample are essentially equal to the allowed energies of an electron in an infinite sample of the same material. Thus according to Eq. (28), $j_r(\hat{R};E)$ represents the sum of our sample's bulk and surface densities of states, each modulated by appropriate transition matrix elements squared; and moreover, all of the information regarding the magnitude of photoelectron escape depths is contained in these matrix elements. Consequently, in the event that the modulation due to photoemission matrix elements is weak, structure observed in $j_r(\hat{R};E)$ can be attributed to the sum of our semi-infinite sample's bulk and surface densities of states.

III. BULK BAND-STRUCTURE EFFECTS: RECOVERY OF THE THREE STEP MODEL

The discussion in this and the following section is aimed at showing how PED's should vary with $\hbar\omega$, according to our quantum theory of photoemission. In the present section we are concerned with the effect on this variation of photoelectron momentum broadening, particularly in the limit that this broadening is small (i.e., where the photoelectron escape depths are long). In this limit we demonstrate the correspondence between our Fermi's Golden-Rule formula, Eq. (28), and the semiclassical three-step model,[20] which is widely used to interpret photoemission data. (The derivation which follows is quite similar to that used by Mahan[6] in recovering the three-step model for the case of a nearly-free-electron solid.)

Generally, one plots a series of photoemission spectra for different photon frequencies (see, e.g., Fig. 1) on a graph whose ordinate

$$\bar{E} \equiv E - \hbar\omega \tag{33}$$

is the binding energy of the electrons which have been photoexcited. Thus, of the two factors which, according to Eq. (28), can give rise to structure in a photoemission spectrum, namely, (a) the spatial distribution and interference of electron and hole wave functions, via the photoexcitation matrix elements

$$\mathfrak{M}(p_n, n; \hat{R}, \bar{E}+\hbar\omega) \equiv \int dz \int_{\Omega_2} d^2\rho\, U^*(\vec{\rho}, z; \hat{R}, \bar{E}+\hbar\omega) \times\left(\vec{\epsilon}_{\parallel}\cdot\vec{k}_{\parallel} + \frac{1}{i}\hat{\epsilon}\cdot\vec{\nabla}\right) V^{(n)}_{\vec{k}_{\parallel}^{(r)},p_n}(\vec{\rho}, z)\,, \tag{34}$$

and (b) the occupied density of states, via the energy-conserving δ function

$$\delta(\bar{E} - E^{(n)}_{\vec{k}_{\parallel}^{(r)},p_n})\,, \tag{35}$$

only the former can give rise to structure which moves with $\hbar\omega$. (This result is self-evident, the argument of the δ function is ω independent.)

Therefore, we focus our attention on the $\mathfrak{M}(p_n, n; \hat{R}, \bar{E}+\hbar\omega)$, and in order to establish the correspondence between Eq. (28) and the usual three-step model, we extract from the $\mathfrak{M}$'s the remnant they contain of crystal-momentum conservation normal to the surface. For this purpose, we turn to the determination of the forms of the $U(\vec{\rho}, z; \hat{R}, \bar{E}+\hbar\omega)$ and $V^{(n)}_{\vec{k}_{\parallel}^{(r)}p_n}(\vec{\rho}, z)$ which enter Eq. (34).

We begin by making use of the fact that a sample's crystal potential, $v(\vec{\rho}, z)$, may generally be assumed only to differ from its bulk form in the sample's outermost atomic layer [or possibly two or three layers, in the case of impurity adsorption or surface rearrangement]. Thus let us choose our origin of coordinates to a layer or so below the sample surface, and assume that for $z \geq 0$, $v(\vec{\rho}, z)$ has completely "healed" to its bulk form.

Then for any $z \geq 0$,

$$v(\vec{\rho}, z) = v(\vec{\rho} + \vec{c}_{\parallel}, z + c_{\perp})\,, \tag{36}$$

where the lattice translation vector $\vec{c} \equiv (\vec{c}_{\parallel}, c_{\perp})$ connects any point $(\vec{\rho}, z)$ to the nearest equivalent point[40] in a deeper layer of the lattice, and the wave functions $U(\vec{\rho}, z; \hat{R}; \bar{E}+\hbar\omega)$ and $V^{(n)}_{\vec{k}_{\parallel}^{(r)},p_n}(\vec{\rho}, z)$, which enter Eq. (34), may be expressed as linear combinations of propagating and evanescent[41] Bloch functions of z. For example U takes the form,

$$U(\vec{\rho}, z; \hat{R}; \bar{E}+\hbar\omega) = \sum_{n''} T_{n''}(\vec{k}_{\parallel}^{(r)}; \bar{E}+\hbar\omega) \times e^{ik_{\perp}(\bar{E}+\hbar\omega, \vec{k}_{\parallel}^{(r)}, n'')z} f_{n''}(\vec{\rho}, z; \vec{k}_{\parallel}^{(r)}; \bar{E}+\hbar\omega)\,, \tag{37}$$

in the reduced zone scheme, where n'' is a three-dimensional band index, and where $f_{n''}(\vec{\rho}, z; \vec{k}_{\parallel}^{(r)}; \bar{E}+\hbar\omega)$ is a periodic function of $\vec{\rho}$ and z [in the same sense as is $v(\vec{\rho}, z)$, cf. Eq. (36)], with the periodicity of the semi-infinite crystal lattice. Since U is a wave function representing a beam of electrons incident on the sample from the vacuum side, the Bloch functions in Eq. (37) are necessarily "outgoing" at $z = \infty$, and therefore the wave vectors $k_{\perp}$, which are in general complex, have non-negative real and imaginary parts. If the crystal potential is assumed to be real, then certain of the $k_{\perp}$ in Eq. (37) may be pure real, corresponding to the transmission of the incident electron beam into the sample in bulk Bloch wave band states. For these $k_{\perp}$, the corresponding constants $T_{n''}(\vec{k}_{\parallel}^{(r)}, \bar{E}+\hbar\omega)$ represent transmission amplitudes. If none of the $k_{\perp}$ in Eq. (37) are real [still assuming $v(\vec{\rho}, z)$ to be nonabsorptive], then the incident electron beam's energy and momentum along the surface correspond to a band gap in the solid's E vs k relation,[42] and the beam suffers total external reflection. If more realistically, $v(\vec{\rho}, z)$ is assumed to have an absorptive (i.e., imaginary) part, representing inelastic electron scattering, then all of the $k_{\perp}$ in Eq. (37) will be complex. The constants $T_{n''}(\vec{k}_{\parallel}^{(r)}, \bar{E}+\hbar\omega)$, we note, can be evaluated by matching at the plane $z = 0$. [Before leaving the U's we wish to emphasize the fact that these wave functions are identical to those which one calculates in the multiple scattering theory of LEED. Thus large computer programs for calculating the U's are available at present. The modification of such programs for the calculation of the $V^{(n)}$'s should not present any particular difficulty, except that an accurate calculation of them will probably require the use of a self-consistent $v(\vec{\rho}, z)$.[43] Evaluations of the self-consistent $v(\vec{\rho}, z)$ together with the corresponding $V^{(n)}$ have recently been carried out, for a few materials: Si,[44] Al,[45] and the alkali metals.[46]]

The form of the expression analogous to Eq. (37) for the occupied state wave functions, $V^{(n)}_{\vec{k}_{\parallel}^{(r)},p_n}(\vec{\rho}, z)$, is different depending on whether $V^{(n)}_{\vec{k}_{\parallel}^{(r)},p_n}(\vec{\rho}, z)$ is supposed to represent a bulk-band state or a surface state. For bulk bands, one has[47]

$$V^{(n)}_{\vec{k}_{\parallel}^{(r)},p_n}(\vec{\rho}, z) = e^{-ip_n(\bar{E}, \vec{k}_{\parallel}^{(r)})z} g_n^-(\vec{\rho}, z; \vec{k}_{\parallel}^{(r)}\bar{E}) + \sum_{n'} C_{nn'}(\vec{k}_{\parallel}^{(r)}, \bar{E}) e^{ip_{n'}(\bar{E}, \vec{k}_{\parallel}^{(r)})z} \times g^+_{n'}(\rho, z; \vec{k}_{\parallel}^{(r)}, \bar{E})\,, \tag{38}$$

while for surface states, one has

$$V^{(n)}_{\vec{k}_{\parallel}^{(r)}}(\vec{\rho}, z) = \sum_{n'} C_{nn'}(\vec{k}_{\parallel}^{(r)}, E) \times e^{ip_{n'}(\bar{E}, \vec{k}_{\parallel}^{(r)})z} g^+_n(\vec{\rho}, z; \vec{k}_{\parallel}^{(r)}, \bar{E})\,. \tag{39}$$

In Eqs. (38) and (39), the reduced zone scheme is used, n and n' are three-dimensional band indices, and the $g_n^{\pm}(\vec{\rho}, z, \vec{k}_{\parallel}^{(r)}, \bar{E})$ are periodic functions of $\vec{\rho}$ and z having the periodicity of the semi-infinite crystal lattice.[48] The amplitudes $C_{nn'}(\vec{k}_{\parallel}^{(r)}, \bar{E})$ are determined by matching at $z=0$.

Recall that in reducing the spectral function $G^+(\vec{x}_1, \vec{x}_2; \bar{E})$ of Eq. (16) to the form

$$2\pi i \sum_{\text{occupied } j} \delta(\bar{E}-E_j)\psi_j(\vec{x}_1)\psi_j^*(\vec{x}_2)$$

in Eq. (17), we made explicit use of the assumption that the crystal potential $v(\vec{\rho}, z)$ be real. Thus although we may assume $v(\vec{\rho}, z)$ to have an energy-dependent imaginary part which is large enough at energy $\bar{E}+\hbar\omega$ to account for the inelastic scattering of outgoing photoelectrons, this imaginary part of v must also be assumed to vanish at the energies $\bar{E}$ of the occupied states.[49] This latter assumption implies that the wave vectors $p_{n'}(\bar{E}, k_{\parallel}^{(r)})$ in Eq. (38) are either pure real (and by convention positive), or complex and of positive imaginary part. The wave vector $p_n(\bar{E}, k_{\parallel}^{(r)})$ is evidently one of the purely real p's. At energies $\bar{E}$ such that no real $p_{n'}(\bar{E}, \vec{k}_{\parallel}^{(r)})$ exist, one is in a band gap, and one searches for surface states, whose wave functions for $z>0$ are as in Eq. (39).

We now make use of Eqs. (37) and (38) to extract the factor in the photoemission matrix element $\mathfrak{M}(p_n, n; \hat{R}, \bar{E}+\hbar\omega)$ [Eq. (34)] which represents the remnant of crystal-momentum conservation normal to the sample surface. Substituting Eqs. (37) and (38) into Eq. (34), we find for photoemission from a bulk band state,

$$\mathfrak{M}(p_n, n; \hat{R}, \bar{E}+\hbar\omega) = \mathfrak{M}_s(p_n, n; \hat{R}, \bar{E}+\hbar\omega) + \sum_{n''} T_{n''}(\vec{k}_{\parallel}^{(r)}; \bar{E}+\hbar\omega)\Big[\Delta^-_{n'',n}(\vec{k}_{\parallel}^{(r)}, \bar{E}, \hbar\omega)M^-_{n'',n}(\vec{k}_{\parallel}^{(r)}, \bar{E}, \hbar\omega) + \sum_{n'} C_{nn'}(\vec{k}_{\parallel}^{(r)}, \bar{E})\Delta^+_{n'',n'}(\vec{k}_{\parallel}^{(r)}, \bar{E}, \hbar\omega)M^+_{n'',n'}(\vec{k}_{\parallel}^{(r)}, \bar{E}, \hbar\omega)\Big] . \tag{40}$$

In Eq. (40), $\mathfrak{M}_s$ represents the contribution to $\mathfrak{M}(p_n, n; \hat{R}, \bar{E}+\hbar\omega)$ from the integration of z between $-\infty$ and 0 [cf. Eq. (34)]. The factors $M^{\pm}_{n'',n'}(\vec{k}_{\parallel}^{(r)}, \bar{E}, \hbar\omega)$ are given by

$$M^{\pm}_{n'',n'}(\vec{k}_{\parallel}^{(r)}, \bar{E}, \hbar\omega) \equiv \int_0^{c_\perp} dz \int_\Omega d^2\rho\, e^{-ik_\perp^*(\bar{E}+\hbar\omega, \vec{k}_{\parallel}^{(r)}, n'')z} f^*_{n''}(\vec{\rho}, z; \vec{k}_{\parallel}^{(r)}; \bar{E}+\hbar\omega) \times\left(\vec{\epsilon}_{\parallel}\cdot\vec{k}_{\parallel}^{(r)} + \frac{1}{i}\hat{\epsilon}\cdot\vec{\nabla}\right)\left[e^{\pm ip_{n'}(\bar{E}, \vec{k}_{\parallel}^{(r)})z} g^{\pm}_{n'}(\vec{\rho}, z; \vec{k}_{\parallel}^{(r)}; \bar{E})\right] , \tag{41}$$

and represent intralayer contributions to the photoexcitation matrix element. Finally, the factors $\Delta^{\pm}_{n'',n'}$ in Eq. (40) are defined by

$$\Delta^{\pm}_{n'',n'}(\vec{k}_{\parallel}^{(r)}, \bar{E}, \hbar\omega) \equiv \left(1-\exp\{ic_\perp[\pm p_{n'}(\bar{E}, \vec{k}_{\parallel}^{(r)}) - k_\perp^*(\bar{E}+\hbar\omega, \vec{k}_{\parallel}^{(r)}, n'')]\}\right)^{-1} ; \tag{42}$$

they represent the interference of the contributions to $\mathfrak{M}$ from the different layers of the sample.

Note that if

$$c_\perp \operatorname{Im} k_\perp(\bar{E}+\hbar\omega, \vec{k}_{\parallel}^{(r)}, n'') \ll 1 , \tag{43}$$

then $\Delta^+_{n'',n'}(\vec{k}_{\parallel}^{(r)}, \bar{E}, \hbar\omega)$ is sharply peaked whenever $\bar{E}$ and $\vec{k}_{\parallel}^{(r)}$ are such that the equation

$$p_{n'}(\bar{E}, \vec{k}_{\parallel}^{(r)}) = \operatorname{Re} k_\perp(\bar{E}+\hbar\omega, \vec{k}_{\parallel}^{(r)}, n'') \tag{44}$$

is satisfied.[50] Equation (44) is, of course, the equation representing crystal-momentum conservation in the z direction. Thus the factors $\Delta^{\pm}_{n'',n'}$ in Eq. (40) represent the remnant of this conservation law in photoemission from a semiinfinite sample. For each set of n'' and n', it is clear that the values of $\bar{E}$ and $\vec{k}_{\parallel}^{(r)}$ at which Eq. (44) is satisfied depend on $\hbar\omega$. Thus the peaks in $\mathfrak{M}(p_n, n; \hat{R}, \bar{E}+\hbar\omega)$ contributed by the $\Delta^+_{n'',n'}(\vec{k}_{\parallel}^{(r)}, \bar{E}, \hbar\omega)$ will move with $\hbar\omega$. [These peaks should give rise to the most important ω-dependent structure in PED's. Therefore one should be able to use the observed ω dependence of PED peak position, heights, and widths in conjunction with model-band calculations to determine the energy-band dispersion relations of the corresponding sample.]

We focus first on the case that Eq. (43) is well satisfied by one or more of the $k_\perp(\bar{E}+\hbar\omega, \vec{k}_{\parallel}^{(r)}, n'')$. In this case, among the various contributions to $|\mathfrak{M}(p_n, n; \hat{R}, \bar{E}+\hbar\omega)|^2$, the largest are from terms which involve $|\Delta^+_{n'',n'}(\vec{k}_{\parallel}^{(r)}, \bar{E}, \hbar\omega)|^2$, since $\Delta^+_{n'',n'}$ and its complex conjugate blow up simultaneously. Therefore, let us ignore cross terms [those involving $\Delta^{+*}_{n'',n'''}\Delta^+_{n'',n'}$, $n'''\neq n'$] and see how the familiar semiclassical model of photoemission can be recovered from Eq. (28), our Fermi's Golden Rule.[51]

From Eq. (42), we obtain the expression,

$$\left|\Delta^{\pm}_{n'',n'}(\vec{k}_{\parallel}^{(r)}, \bar{E}, \hbar\omega)\right|^2 = \left((1-e^{-c_\perp k_\perp^{(2)}(n'')})^2 + 4e^{-c_\perp k_\perp^{(2)}(n'')}\sin^2\{\tfrac{1}{2}c_\perp[k_\perp^{(1)}(n'') - p_{n'}(\bar{E}, \vec{k}_{\parallel}^{(r)})]\}\right)^{-1} , \tag{45}$$

in which $k_\perp^{(1)}(n'')$ and $k_\perp^{(2)}(n'')$ are, respectively, the real and imaginary parts of $k_\perp(\bar{E}+\hbar\omega, \vec{k}_\parallel^{(r)}, n'')$, and, of course, $p_{n'}(\bar{E}, \vec{k}_\parallel^{(r)})$ is one of the set of p's which are real (and positive). However, we are only interested in the contributions of the peaks of $|\Delta^+_{n'',n'}|^2$. Therefore we reduce Eq. (45) to the approximate form,

$$|\Delta^+_{n'',n'}(\vec{k}_\parallel^{(r)}, \bar{E}, \hbar\omega)|^2 \approx \frac{1}{c_\perp^2} \times \sum \frac{1}{[k_\perp^{(2)}(n'')]^2 + [k_\perp^{(1)}(n'') - p_{n'}(\bar{E}, \vec{k}_\parallel^{(r)})]^2} \ , \tag{46}$$

in which the heights and half-widths of the peaks are seen to equal $[c_\perp k_\perp^{(2)}(n'')]^{-2}$ and $k_\perp^{(2)}(n'')$, respectively. In the limit that $k_\perp^{(2)}(n'')$ approaches zero, Eq. (46) may be written

$$|\Delta^+_{n'',n'}(\vec{k}_\parallel^{(r)}, \vec{E}, \hbar\omega)|^2 \approx [\pi/c_1^2 k_1^{(2)}(n'')] \times \delta(k_\perp^{(1)}(n'') - p_{n'}(\bar{E}, \vec{k}_\parallel^{(r)})) \ . \tag{47}$$

We now substitute Eq. (40) into Eq. (28), ignore all cross terms and terms involving $\mathfrak{M}_s$ or $\Delta^-_{n'',n}$, make use of Eq. (47), and finally, we take advantage of the theorem

$$\sum_{\substack{n;\\ \text{occupied}}} \left| \frac{dE^{(n)}_{\vec{k}_\parallel^{(r)}, p_n}}{dp_n} \right|^{-1} |C_{n,n'}(\vec{k}_\parallel^{(r)}, E)|^2 = \left| \frac{dE^{(n')}_{\vec{k}_\parallel^{(r)}, p_{n'}}}{dp_{n'}} \right|^{-1} \tag{48}$$

which is a consequence of current conservation and the principle of detailed balance,[52] for values of n' such that $p_{n'}(\bar{E}, \vec{k}_\parallel^{(r)})$ is real. We thereby arrive at the approximate expression for the photocurrent,

$$R^2 j_r(\hat{R}, \bar{E}+\hbar\omega) \approx 2e\mathfrak{F}S \frac{\alpha a_B}{\pi|\vec{\epsilon}_\parallel|} \frac{[\Re(\bar{E}+\hbar\omega)]^{1/2}}{(\hbar\omega)^2} \sum_{n''} |T_{n',r}(\vec{k}_\parallel^{(r)}; \bar{E}+\hbar\omega)|^2 \times \sum_{n'} \frac{\pi}{c_\perp^2 k_\perp^{(2)}(n'')} \delta(k_\perp^{(1)}(n'') - p_{n'}(\bar{E}, \vec{k}_\parallel^{(r)})) \left| \frac{dE^{(n')}_{\vec{k}_\parallel^{(r)}, p_{n'}}}{dp_{n'}} \right|^{-1} |M^+_{n'',n'}(\vec{k}_\parallel^{(r)}, \bar{E}, \hbar\omega)|^2 \ , \tag{49}$$

in which the sum on n' is restricted to values such that $p_{n'}(\bar{E}, \vec{k}_\parallel^{(r)})$ is real, and the sum on n'' includes only those values for which Eq. (43) is well satisfied.

Since we have already assumed $k_\perp^{(2)}(n'')$ to be small in evaluating the contribution of $|\Delta^+_{n'',n'}|^2$ to Eq. (49), it would seem reasonable to neglect it as well in evaluating $M^+_{n'',n'}(\vec{k}_\parallel^{(r)}, \bar{E}, \hbar\omega)$ [via Eq. (41)]. In this approximation, however, $M^+_{n'',n'}$ is just the integral over a unit cell of $(1/i)\hat{\epsilon}\cdot\vec{\nabla}$ sandwiched between initial and final Bloch wave functions, which carry no information regarding the existence of a surface.

Thus only $[k_\perp^{(2)}(n'')]^{-1}$ and $|T_{n',r}(\vec{k}_\parallel^{(r)}, \bar{E}+\hbar\omega)|^2$ carry surface information in the small-$k_\perp^{(2)}(n'')$ approximation. The photoelectron escape depth is represented by $[k_\perp^{(2)}(n'')]^{-1}$ itself; that is, $(k_\perp^{(2)})^{-1}$ equals the average depth from which a photoelectron can travel to the sample surface without suffering an inelastic collision.[53] The probability that an electron which arrives at the surface will be transmitted into the vacuum is represented by $|T_{n',r}(\vec{k}_\parallel^{(r)}, \bar{E}+\hbar\omega)|^2$, in Eq. (49). [Although $|T_{n',r}|^2$ is actually a coefficient for transmission of an electron into the solid from the vacuum, the law of detailed balance relates such a coefficient to one for transmission in the other direction (cf. Eq. (51) below).]

We see, therefore, that Eq. (49) represents photoemission as a three-step process: photoexcitation treated as a bulk process, transport to the surface without energy loss of electrons that were photoexcited within an average depth $[k_\perp^{(2)}(n'')]^{-1}$ below it, and transmission into the vacuum. Equation (49) is, therefore, precisely a "three-step model" formula for the angle-resolved photocurrent, $j_r(\hat{R}, \bar{E}+\hbar\omega)$.

From Eq. (49) it is straightforward to obtain the corresponding formula for the angle-integrated current, $J_r(\bar{E}+\hbar\omega)$. One has

$$J_r(\bar{E}+\hbar\omega) \equiv \int d\hat{R}\, j_r(\hat{R}, \bar{E}+\hbar\omega) = \left[\frac{2m}{\hbar^2}(\bar{E}+\hbar\omega)\right]^{-1/2} \times \int d^2k_\parallel \frac{\Theta[(2m/\hbar^2)(\bar{E}+\hbar\omega) - k_\parallel^2]}{[(2m/\hbar^2)(\bar{E}+\hbar\omega) - k_\parallel^2]^{1/2}} j_r(\hat{R}, \bar{E}+\hbar\omega) \ . \tag{50}$$

For the sake of comparison with the usual three-step model, we make use of the relation between the $|T_{n',r}(\vec{k}_\parallel^{(r)}, \bar{E}+\hbar\omega)|^2$ and the probability, $P(n'', \vec{k}_\parallel^{(r)}, \bar{E}+\hbar\omega \to \vec{k}_\parallel, \bar{E}+\hbar\omega)$, for a Bloch electron arriving at the surface with quantum numbers n'', $\vec{k}_\parallel^{(r)}$, $\bar{E}+\hbar\omega$ to be transmitted into the vacuum in the plane-wave state

$$\exp\{i\vec{k}_\parallel\cdot\vec{\rho} - i[(2m/\hbar^2)(\bar{E}+\hbar\omega) - k_\parallel^2]^{1/2} z\}.$$

According to the law of detailed balance, this relation is given as[54]

$$P(n'', \vec{k}_{\parallel}^{(r)}, \bar{E}+\hbar\omega \rightarrow \vec{k}_{\parallel}, \bar{E}+\hbar\omega) = \frac{v_g^{\perp}(n'', \vec{k}_{\parallel}^{(r)}, \bar{E}+\hbar\omega)}{v_0^{\perp}(\vec{k}_{\parallel}, \bar{E}+\hbar\omega)} \left| T_{n''}(\vec{k}_{\parallel}^{(r)}, \bar{E}+\hbar\omega) \right|^2 , \tag{51}$$

where $v_g^{\perp}$ is

$$v_g^{\perp}(n'', \vec{k}_{\parallel}^{(r)}, \bar{E}+\hbar\omega) \equiv \left| \frac{dE^{(n'')}_{\vec{k}_{\parallel}^{(r)}, k_{\perp}^{(1)}(n'')}}{dk_{\perp}^{(1)}(n'')} \right| , \tag{52}$$

and represents the Bloch wave group velocity along the surface normal, where $v_0^{\perp}(\vec{k}_{\parallel}, \bar{E}+\hbar\omega)$ is defined by

$$v_0^{\perp}(\vec{k}_{\parallel}, \bar{E}+\hbar\omega) = [(2/m)(\bar{E}+\hbar\omega) - (\hbar\vec{k}_{\parallel}/m)^2]^{1/2} , \tag{53}$$

and represents the normal velocity associated with the plane wave. Substituting Eqs. (51) and (49) into Eq. (50) and recalling the identity

$$\left| \frac{dE^{(n)}_{\vec{k}_{\parallel}^{(r)}, K}}{dK} \right|^{-1}_{E^{(n)}_{\vec{k}_{\parallel}^{(r)}, K} = \mathcal{E}} \equiv \int dK\, \delta(\mathcal{E} - E^{(n)}_{\vec{k}_{\parallel}^{(r)}, K}) \Theta(\pm K) , \tag{54}$$

we find the expression for $J_r(\bar{E}+\hbar\omega)$,

$$\begin{aligned} R^2 J_r(\bar{E}+\hbar\omega) = 4e\mathcal{F}S \frac{\alpha}{|\vec{\epsilon}_{\parallel}|} \left(\frac{\mathcal{R}}{\hbar\omega}\right)^2 \frac{a_B^4}{c_{\perp}^2} \sum_{n'', n'} \int d^2k_{\parallel}\, \Theta\left(\frac{2m}{\hbar^2}(E+\hbar\omega) - k_{\parallel}^2\right) \\ \times \int dK\, \Theta(K) \frac{1}{k_{\perp}^{(2)}(n'')} P(n'', \vec{k}_{\parallel}^{(r)}, \bar{E}+\hbar\omega \rightarrow \vec{k}_{\parallel}, \bar{E}+\hbar\omega) \\ \times \delta(\bar{E}+\hbar\omega - E^{(n'')}_{\vec{k}_{\parallel}^{(r)}, K}) \delta(\bar{E} - E^{(n')}_{\vec{k}_{\parallel}^{(r)}, K}) \left| M^{+}_{n'', n'}(\vec{k}_{\parallel}^{(r)}, \bar{E}, \hbar\omega) \right|^2 . \end{aligned} \tag{55}$$

The $\Theta(\pm K)$ in Eq. (54) is necessary in order that we satisfy the δ function for only one sign of K.[55]

We convert Eq. (55) into its final form by making use of the equivalence,

$$\int d^2k_{\parallel} \Longleftrightarrow \sum_{\vec{G}_{\parallel}} \int_{\text{2D BZ}} d^2k_{\parallel}^{(r)} \tag{56}$$

Substituting Eq. (56) into Eq. (55), we obtain the formula[56]

$$\begin{aligned} R^2 J_r(\bar{E}+\hbar\omega) = 4e\mathcal{F}S \frac{\alpha}{|\vec{\epsilon}_{\parallel}|} \left(\frac{\mathcal{R}}{\hbar\omega}\right)^2 \frac{a_B^4}{c_{\perp}^2} \sum_{n'' n'} \sum_{\vec{G}_{\parallel}} \int_{\text{BZ}/2} d^2k_{\parallel}^{(r)}\, dK \\ \times \Theta\left(\bar{E}+\hbar\omega - \frac{\hbar^2(\vec{k}_{\parallel}^{(r)} + \vec{G}_{\parallel})^2}{2m}\right) \frac{1}{k_{\perp}^{(2)}(n'')} P(n'', \vec{k}_{\parallel}^{(r)}, \bar{E}+\hbar\omega \rightarrow \vec{G}_{\parallel} + \vec{k}_{\parallel}^{(r)}, \bar{E}+\hbar\omega) \\ \times \delta(\bar{E}+\hbar\omega - E^{(n'')}_{\vec{k}_{\parallel}^{(r)}, K}) \delta(\bar{E} - E^{(n')}_{\vec{k}_{\parallel}^{(r)}, K}) \left| M_{n'', n'}(\vec{k}_{\parallel}^{(r)}, \bar{E}, \hbar\omega) \right|^2 . \end{aligned} \tag{57}$$

Apart from the sum on $\vec{G}_{\parallel}$, Eq. (57) is identical[53] to the usual semiclassical three-step model formula for $J_r(\bar{E}+\hbar\omega)$. The sum on $\vec{G}_{\parallel}$ represents the fact that since momentum parallel to the surface is only conserved to within a two-dimensional reciprocal lattice vector, a Bloch wave of crystal momentum $\vec{k}_{\parallel}^{(r)}$ can be transmitted into the vacuum in any of a number of beams, i.e., those with $\vec{k}_{\parallel}$ equal to $\vec{k}_{\parallel}^{(r)} + \vec{G}_{\parallel}$. In the usual semiclassical formulation one ignores this possibility, but only for the sake of convenience. If one took it into account, the semiclassical formula and Eq. (57) would agree exactly.

Let us turn, finally, to the question of actual calculations of photocurrents using the formulas we have derived. First, we notice that momentum conservation structure is much sharper and more pronounced in the angle-resolved photocurrent $j_r(\hat{R}, \bar{E}+\hbar\omega)$ [where, cf., Eq. (49), it is δ-function-like] than in the angle-integrated current $J_r(\bar{E}+\hbar\omega)$ [where, cf. Eq. (57), it is of the form of critical-point singularities in the energy distribution of joint density of states[57,58]]. The reason for this difference is clear; if one observes at fixed $\hat{R}$, two more selection rules, conservation of each of the components of $\vec{k}_{\parallel}^{(r)}$, can prevent one from seeing a photoelectron than if one observes at all angles. We therefore conclude the following: (a) In order to use photoemission spectra to determine a sample's bulk density of states, one should measure angle-integrated photocurrents which are less strongly modulated by momentum-conservation structure. (b) Conversely, in order to obtain detailed band-structure information it will be useful to observe

photoemission as a function of $\hat{R}$ (assuming specular surfaces can be achieved). (c) In the case that one sees sharp well-separated peaks in angle-resolved PED's, one should be able to deduce from their widths, the electron inelastic mean free paths, $[k_\perp^{(2)}(n'')]^{-1}$, which are not otherwise easily measurable. This result follows if one uses the more realistic expression for the $|\Delta^+_{n'',n'}(\vec{K}_\parallel^{(r)}, \bar{E}, \hbar\omega)|^2$, Eq. (46), rather than that of Eq. (47) to obtain a formula for $j_r(\hat{R}, \bar{E}+\hbar\omega)$.

In the important energy range 20 eV $\lesssim \bar{E}+\hbar\omega$ which is less than a few 10^2 eV, for most materials, electron mean free paths are known[4,59,60] to be quite short. In this regime, therefore, it is altogether inappropriate to make use of the approximation that the $k_\perp^{(2)}(n'')\approx 0$. In order to calculate photocurrents for these energies one must return to Eq. (40), for $\mathfrak{M}(p_n, n; \hat{R}, \bar{E}+\hbar\omega)$, and substitute it into Eq. (28). In such a calculation, surface effects become important. These effects are qualitatively discussed in Sec. IV.

IV. QUALITATIVE DESCRIPTION OF PHOTOEMISSION FOR SEVERAL REGIMES

In this section, we describe the trend from the ultraviolet photoemission (or "band structure") regime described in Sec. III to the x-ray photoemission (or "density-of-states") regime. In an independent-particle description, this gradual transition depends on (a) the $\vec{k}$-dependent escape depths of the emerging photoelectrons, (b) the coherence lengths of the holes which are created, and (c) the increasing number of final-state energy bands at higher electron energies. We also describe the "band gap" case of directional photoemission in which the final-state LEED wave function has no propagating Bloch-like component in the solid but only rapidly decaying evanescent ones. In this case, the surface contribution to the photocurrent becomes enhanced relative to that of the "bulk." Photoemission from localized intrinsic and extrinsic (e.g., adsorbate) surface states are also briefly described.

A. "Bulk" ultraviolet photoemission spectroscopy (UPS) and x-ray photoemission spectroscopy (XPS) limits

In Sec. III, conservation of crystal momentum was shown to depend on the existence of sufficiently weak damping [Eq. (43)], i.e., a sufficiently large attenuation depth $(k_\perp^{(2)})^{-1}$. In this case, which is often satisfied in the ultraviolet photoemission regime at low photon energies, $\hbar\omega$-dependent structure is observed in the PED's which reflects structure in the energy distribution of the joint density of states (EDJDOS).[2-4] This "direct interband transition" case is schematically shown in Fig. 5(a). However, the existence of weak damping [Eq. (43)] is a necessary but not sufficient condition for PED's to reflect structure in the EDJDOS. That is, it is well known that XPS primarily measures structure in the single-particle density of states (DOS) rather than the EDJDOS, even though the weak-damping condition [Eq. (43)] is well satisfied.[60] The latter occurs because the density of available final states which conserve both energy and momentum becomes sufficiently large, relative to the momentum broadening $k_\perp^{(2)}$, that all initial states can be excited.

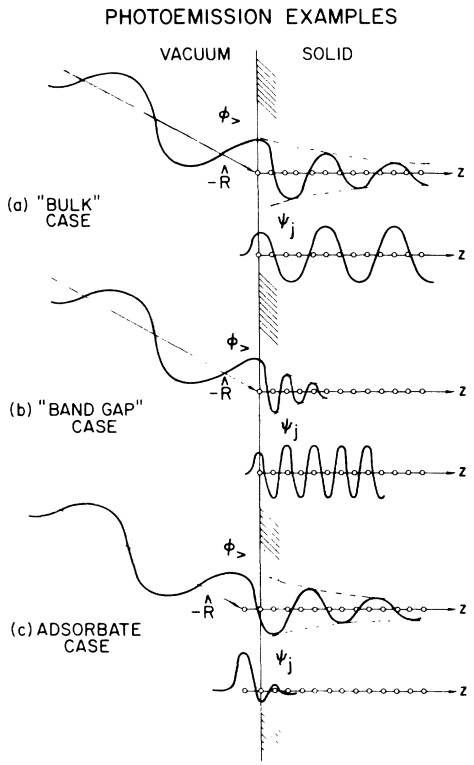

FIG. 5. (a) Schematic diagram of the initial-state wave function Ψ_j and final-state wave function $\phi_>$ involved in direct interband transitions for the care of "bulk" photoemission from a semi-infinite solid. (b) Schematic diagram for the band-gap case in which the final-state wave function $\phi_>$ corresponds to a band gap in the solid and thus within the solid consists only of rapidly decaying surface evanescent waves. (c) Schematic diagram of Ψ_j and $\phi_>$ for the case of an adsorbate with localized initial-state wavefunctions Ψ_j.

To show this trend from the UPS to the XPS regime qualitatively, we consider a nearly-free-electron (NFE) model. For this model the density of final states per unit volume varies as $\rho(E) = 1.5E^{1/2}/E_{BZ}^{3/2}$ and the average band width of each band (reduced-zone scheme) is $W \simeq (2\hbar^2E/m)^{1/2}k_{BZ}$. Here k_{BZ} is the Brillouin-zone momentum and we have normalized to one state for $E = E_{BZ} = \hbar^2k_{BZ}^2/2m$. Thus the number of bands $N_B(E)$ at energy E is $N_B(E) \simeq \rho(E)W = 3E/E_{BZ}$. Since each band passes through one $k_\perp$ point for each $\vec{K}_\parallel$, the average sepa-

ration $\delta k_\perp$ of available $k_\perp$ states at an energy E is

$$\delta k_\perp \simeq k_{BZ}/N_B = E_{BZ}k_{BZ}/3E \ . \tag{58}$$

A criterion for the XPS limit is the existence of a "quasicontinuum" of final states such that all initial states can be excited, that is,

$$\delta k_\perp \lesssim k_\perp^{(2)}(\bar{E}+\hbar\omega, \vec{k}_\parallel^{(r)}, n'') \ , \tag{59}$$

namely, if the average separation $\delta k_\perp$ of available $k_\perp$ states at energy $E=\bar{E}+\hbar\omega$ is less than the broadening $k_\perp^{(2)}$, then all initial states at energy $\bar{E}$ (any $k_\perp$) are excited with equal probability so far as phase space is concerned. The above criterion is valid for the case of polycrystalline samples, and possibly for the case of angle-integrated photoemission from single crystals at moderate-to-high energies. The available final-state phase space becomes smaller (i.e., $\delta k_\perp$ becomes larger) for the case of photoemission from single crystals at low energies, especially of course, for angle-resolved photoemission.

In Fig. 6, we show the typical range of values[59,61] of $k_\perp^{(2)}(E)$ for most materials, where $k_\perp^{(2)}(E)=\lambda_{ee}^{-1}$ for electrons emitted normal to the surface. Also shown in Fig. (6) is $\delta k_\perp(E)$ for a NFE model. Here we have used $a=4$ Å and an inner potential $V_0 \sim 8$ eV. As shown in Fig. 6, the XPS limit [Eq. (59)] is typically reached for $\hbar\omega \gtrsim 20$ to 40 eV, the exact value depending on the electron escape depth $\lambda_{ee}=(k_\perp^{(2)}\cos\theta)^{-1}$, crystal structure, etc. (here $\cos\theta$ is the direction cosine of the electron momentum relative to the surface normal). This result is consistent with photoemission measurements for polycrystalline Au[10,13] (Fig. 1) as well as for many other materials that have been studied.[62] While structures in PED's tend to have invariant binding energies in the XPS limit, relative peak heights and peak shapes are often frequency dependent due to characteristic frequency-dependent dipole matrix elements [Eq. (40)], for various s, p, d, and f states. These frequency dependences are often large in the $15 \lesssim \hbar\omega \lesssim 100$-eV range and can sometimes be used to identify the character of various valence states,[63] as well as the partial densities of states.

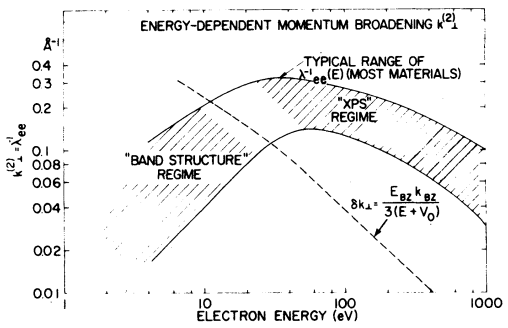

FIG. 6. Illustration of the trend from the band-structure photoemission regime (with direct interband transitions) at low electron energies to the XPS or photoemission-density-of-states regime, at high photon energies. These regimes are defined by $k_\perp^{(2)} < \delta k_\perp$ and $k_\perp^{(2)} > \delta k_\perp$, respectively. Here $k_\perp^{(2)}$ is the electron momentum broadening normal to the surface ($k_\perp^{(2)}=\lambda_{ee}^{-1}$ for electrons emitted normal to the surface) and $\delta k_\perp$ is the average momentum separation normal to the surface of available $k_\perp$ states at an energy E for polycrystalline samples. The shaded region shows the typical range of $k_\perp^{(2)}=\lambda_{ee}^{-1}$ for most materials (Refs. 59 and 60).

Returning now to the UPS band-structure regime, an additional criterion for PED's to reflect structure in the EDJDOS is that the initial hole state have a sufficiently long coherence length, i.e., a sufficiently small momentum broadening $\Delta p_\perp$. On dimensional grounds, it is clear that the criterion for hole states to be well defined is of the form

$$c_\perp \Delta p_\perp(\bar{E}, k_\parallel^{(r)}, n') \ll 1 \ . \tag{60}$$

Typically, this criterion is well satisfied for extended hole states near the top of the valence band but can be violated for strongly damped hole states such as the lowest valence s-band states in covalent semiconductors (e.g., Si, Ge). Hole states which are localized by virtue of a narrow bandwidth also violate this criterion.

We can now summarize criteria for the XPS and "band-structure" regimes. The main criterion for the XPS regime, i.e., for PED's to reflect structure in the DOS (weighted by transition probabilities), is given by Eq. (59) for the case of polycrystalline specimens. In this regime, well-defined $\vec{k}$-conserving transitions [Eq. (43)] usually occur for $\hbar\omega \gtrsim 50$ eV. The criteria for the "band structure" regime, e.g., for PED's to reflect structure in the EDJDOS are more stringent and are given by

$$\text{(a)} \quad c_\perp \Delta p_\perp(\bar{E}, \vec{k}_\parallel^{(r)}, n'') \ll 1 \ , \tag{60}$$

$$\text{(b)} \quad k_\perp^{(2)}(\bar{E}+\hbar\omega, \vec{k}_\parallel^{(r)}, n'') < \delta k_\perp \ , \tag{61}$$

where $k_\perp^{(2)}=(\lambda_{ee}\cos\theta)^{-1}$ and $\delta k_\perp$ is crudely given by Eq. (58). [Note that Eq. (61) automatically implies the satisfaction of Eq. (43), the final state condition for the existence of direct interband transitions.]

While discussing the "band-structure" regime, it is worthwhile to point out that the damping constant $k^{(2)}(\bar{E}+\hbar\omega, \vec{k}_\parallel^{(r)}, n'')$ depends on the band structure, as has been previously noted.[64,65] In particular, in the "random-$\vec{k}$" or "phase-space" approximation,[66] the inelastic scattering length $\lambda_{ee}=(k_\perp^{(2)}\cos\theta)^{-1}$ is

$$\lambda_{ee}(\bar{E}+\hbar\omega, \vec{k}_\parallel^{(r)}, n'') = \frac{\tau(\bar{E}+\hbar\omega)}{\hbar}\left|\frac{\partial E_{n''}(\vec{k})}{\partial \vec{k}}\right| \ , \tag{62}$$

where the lifetime τ (see Ref. 66) is a slowly varying function of the electron energy E while the

group velocity $\vec{v}=\hbar^{-1}(\partial E/\partial\vec{k})$ is anisotropic and can vary rapidly. The $\vec{k}$ dependence of $k_\perp^{(2)}$ can significantly modulate structure in the PED.

B. Direction "band-gap" photoelectron emission

An interesting special case is that of angular-resolved photoemission from a single crystal surface with conditions such that the final-state LEED wave function $\phi_>$ with energy E and parallel momentum $\vec{k}_\parallel^{(r)}$ corresponds to a band gap for all $k_\perp$ in the solid. In this case, $\phi_>$ within the solid consists only of surface evanescent waves which rapidly decay into the solid [see Fig. 5(b)] with a decay length λ_{gap}. For these conditions, only wave functions within a small distance $\sim\lambda_{gap}$ of the surface contribute to the photocurrent, and the surface contribution (e.g., emission from occupied "intrinsic" surface states or adsorbate surface states) becomes greatly enhanced relative to the usual "bulk" contribution.

We wish to estimate crudely the decay length $\lambda_{gap}^{(E)}$ of the evanescent wave, which corresponds to a momentum broadening $k_{gap}^{(2)}$. For this purpose we use a 2-orthogonalized-plane-wave model, with a Brillouin-zone band gap $E_{gap}=2V_0$ centered at $E_{BZ}=\hbar^2k_{BZ}^2/2m$. For electron energies E in the gap, $E_{BZ}-V_0<E<E_{BZ}+V_0$, we obtain an evanescent wave solution with a complex wave vector $k=k_{BZ}+ik_{gap}^{(2)}$ with

$$k_{gap}^{(2)}(E)=(2m/\hbar^2)^{1/2}[(4EE_{BZ}+V_0^2)^{1/2}-(E+E_{BZ})]^{1/2}\,. \tag{63}$$

As an illustrative example, we consider the W (110) face studied by Feuerbacher *et al.*,[9,14] which has a [110]- direction band gap extending from about 6–11 eV above the Fermi energy E_F. For our crude model, we take $V_0=\frac{1}{2}E_{gap}=2.5$ eV and $E_{BZ}=8.5$ eV. Equation (63) then yields $k_{gap}^{(2)}(E)\simeq 0.51[(34E+6.25)^{1/2}-8.5E]^{1/2}$ Å^{-1} for energies (in eV) in the gap $6<E<11$ eV. To lowest order, the momentum broadening due to inelastic electron-electron scattering $k_\perp^{(2)}$ and to the evanescent wave decay $k_{gap}^{(2)}$ are additive:

$$k_{tot}^{(2)}(E)\simeq k_\perp^{(2)}(E)+k_{gap}^{(2)}(E)\,. \tag{64}$$

As is well known in LEED (and seen in Eq. (64)), band gaps cease to exist for finite damping $k_\perp^{(2)}>0$. Rather, these energy regions correspond to regions of enhanced electron reflection from the surface with enhanced attenuation within the solid.

In Fig. 7, we estimate crudely the final-state total attenuation length $\lambda_{tot}=(k_{tot}^{(2)})^{-1}$ for photoemitted electrons normal to the (110) surface of W. We have used Eq. (64) and have assumed a constant $\lambda_{ee}\simeq 6$ Å for $5\lesssim E\lesssim 15$ eV, which is only a rough guess based on experimental observations of a very short mean free path λ_{ee} for W in general in this energy range.[62] Note in Fig. 7 that even if the damping due to electron-electron scattering is large (e.g., $\lambda_{ee}\sim 6$ Å), damping is significantly increased in the gap region ($\lambda_{tot}\simeq 3$ Å at 8.5 eV) due to the evanescent wave decay. Thus the main contribution to the photocurrent $R^2j_r(\hat{R},E)$ for E in the gap is given by the outermost couple of layers at the surface. It is worth noting the implication of this result vis-á-vis attempts to correlate photoemission data with a surface "local density of states." Since even in the center of the gap, $\lambda_{tot}\approx$ two layers, it appears as if such data will correlate with the non-local density of states, (i.e., $G^+(\vec{x}_1,\vec{x}_2;\vec{E})$ averaged properly over this distance [cf. Eq. (16)] and not with the local state density [defined as $G^+(x_1,x_1;E)$]. Stated another way, photoemission samples all occupied states (surface and bulk for the semi-infinite solid which conserve energy [see Eq. (17)], with each state $|\psi_j\rangle$ being weighted by its transition probability $|\langle\phi_>|0.5(\vec{A}\cdot\vec{P}+\vec{P}\cdot\vec{A})\times|\psi_j\rangle|^2$.

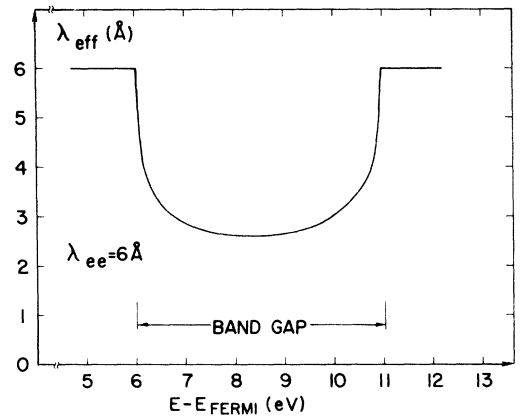

FIG. 7. Schematic diagram of the effective inelastic mean free path λ_{eff} for the band-gap case of photoemission. A constant bulk $\lambda_{ee}=6$ Å has been assumed, with a 5-eV band gap extending from 6 to 11 eV above the Fermi energy E_F (see text).

Quantitative calculations of band-gap emission can be made using Eqs. (28) and (40) and appropriate LEED-type band calculations. Such "band-gap" photoemission studies are interesting in that the surface sensitivity of photoemission spectroscopy (PES) can be enhanced and it appears to be possible in favorable cases to sort out surface and bulk states by varying $\hbar\omega$ such that E passes through a gap region for an initial state in question.

C. Photoemission from adsorbate surface states

We consider the case of localized adsorbate surface states, as schematically shown in Fig. 5(c).

Examples of such states include inorganic (e.g., O, CO) or organic (e.g., C_2H_2, C_6H_6) adsorbates on surfaces for the case when adsorbate energy levels are not degenerate with substrate energy levels. When the adsorbate wave function (or adsorbate-induced "surface-molecule" wave function) is largely confined to the adsorbate layer of thickness $d \sim 2r_0$, where r_0 = adsorbate radius, it has a momentum spread $\delta k_\perp \sim 2\pi/d$ and we expect no strong $\hbar\omega$-dependent changes in the corresponding adsorbate-derived peak locations in the spectra. Thus, to a first approximation, the spectral distribution of ionization energies for an adsorbate surface state can be measured using photoemission.

However, an independent-particle picture is not valid when the initial state is localized as we have assumed; that is, significant many-electron relaxation effects can occur in the photoemission process manifesting the breakdown of Koopmans's theorem. Examples include initial- and final-state polarization effects, image-charge-screening effects, shake-up processes, and multiplet-structure effects. For instance, polarization effects and final-state image-charge screening reduce the ionization energies of an adsorbed molecule relative to the corresponding gas-phase ionization energies.[67–70] Also, significant final-state hole multiplet structure can occur for localized hole states, i.e., the hole state can be left in an excited electronic state such as an excited angular-momentum state.[71–73] Thus, since photoemission never measures the ground state directly but rather leaves the solid in an excited state, it can never measure the local density of states which one would calculate in an independent electron approximation. (This statement is equally true for surface levels, e.g., those associated with an adatom, and for bulk states, e.g., ordinary core levels.)

Regarding the interpretation of photoemission data for adsorbates, one must also consider the effects of final-state interactions. In particular, multiple-beam and final-state interference effects (contained in $\phi_>$) induced by the adsorbate can also affect detailed line shapes and relative $\hbar\omega$-dependent peak amplitudes. Limited experimental evidence to date given by spectra taken with large collection angles suggests that such effects are small.

We turn, finally, from an interpretation of spectral features associated with adsorbate levels to a discussion of their amplitudes. Specifically, in addition to its importance in determining the nature of photoemission spectra, the electron damping length $(k_\perp^{(2)})^{-1}$, or effective mean free path, plays an important role in determining the sensitivity of photoemission spectroscopy as a surface tool. A measure of surface sensitivity is I_S/I_B, the ratio of surface-to-bulk emission intensities. For an adsorbate layer of thickness d, we can roughly estimate

$$I_S/I_B \approx d k_\perp^{(2)} \sigma_S(\omega)/\sigma_B(\omega) , \tag{65}$$

where $\sigma_S(\omega)$ and $\sigma_B(\omega)$ are the absorption cross sections for surface and bulk excitations. As is obvious, surface sensitivity is further enhanced when the adsorbate levels are nondegenerate with the bulk levels. Equation (15) readily shows that surface sensitivity is enhanced for large $k_\perp^{(2)}$, i.e., short mean free paths, which typically occur for energies of $15 \lesssim E \lesssim 100$ eV (Fig. 6). However, $\sigma_S(\omega)$ and $\sigma_B(\omega)$ often have energy-dependent variations which are stronger than those of $k_\perp^{(2)}$. In these cases the energy range for optimum surface sensitivity may be determined by these $\sigma(\omega)$'s rather than by $k_\perp^{(2)}$. For example, many adsorbates of interest have s- and p-derived valence orbitals while many substrates of interest have valence d electrons. In this case the ratio $\sigma_S(\omega)/\sigma_B(\omega)$ has a strong frequency dependence[63] and is often largest for low energies $\hbar\omega \lesssim 20$ eV, depending in detail on the nature of the initial states $|\psi_j\rangle$ involved.

ACKNOWLEDGMENT

We wish to thank W. D. Grobman for many useful discussions.

*Work supported in part by the National Science Foundation under Grant No. H039314 and the Air Force Office of Scientific Research under Contract F44620-70-C-

†Present address: Sandia Labs., Albuquerque, N.M. 87115.

[1]L. Apker, E. Taft, and J. Dickey, Phys. Rev. 74, 1462 (1948).

[2]C. N. Berglund and W. E. Spicer, Phys. Rev. 136, A1030 (1964); 136, A1044 (1964).

[3]N. V. Smith, Crit. Rev. Solid State Sci. 2, 45 (1971).

[4]D. E. Eastman, in *Techniques of Metals Research VI*, edited by E. Passaglia (Interscience, New York, 1972), pp. 413–479.

[5]D. E. Eastman, in *Proceedings of the International Conference on Electron Spectroscopy, Asilomar, CA*, 1971, edited by D. Shirley (North-Holland, Amsterdam, 1972), p. 487.

[6]G. D. Mahan, Phys. Rev. B 2, 4334 (1970).

[7]T. Gustafsson, P. O. Nilsson, and L. Wallden, Phys. Lett. 27A, 121 (1971).

[8]W. E. Spicer, J. Phys. (Paris) 34, C6-19 (1973).

[9]B. Feuerbacher and B. Fitton, Phys. Rev. Lett. 29, 786 (1972).

[10]M. Campagna, D. T. Pierce, K. Sattler, and H. C. Siegman, J. Phys. (Paris) 34, C6-87 (1973), and references therein.

[11]D. E. Eastman and W. D. Grobman, Phys. Rev. Lett.

28, 1327 (1972).
[12]N. V. Smith and M. M. Traum, Phys. Rev. Lett. 31, 1247 (1973).
[13]J. Freeouf, M. Erbudak, and D. E. Eastman, Solid State Commun. 13, 771 (1973).
[14]N. E. Christensen and B. Feuerbacher, Phys. Rev. B 10, 2439 (1974); B. Feuerbacher and N. E. Christensen, *ibid.* 10, 2373 (1974).
[15]C. Caroli, D. Lederer-Rozenblatt, B. Roulet, and D. Saint-James, Phys. Rev. B 8, 4552 (1973).
[16]I. Adawi, Phys. Rev. 134, A788 (1964).
[17]W. L. Schaich and N. W. Ashcroft, Solid State Commun. 8, 1959 (1970); Phys. Rev. B 3, 2452 (1971).
[18]J. Endriz, Phys. Rev. B 7, 3464 (1973).
[19]D. Penn, Phys. Rev. Lett. 28, 1041 (1972).
[20]The "three-step model" of volume photoemission consisting of bulk optical excitations followed by subsequent electron transport to the surface and escape through the surface dates back to at least 1945. Significant contributions to this model include: H. Y. Fan, Phys. Rev. 68, 43 (1945); Ref. 1; W. E. Spicer, Phys. Rev. 112, 114 (1958); H. Thomas, in *Proceedings of the International Symposium on Basic Problems in Thin Physics, Clausthal-Gottingen*, 1965 (Vandenhoek and Ruprecht, Gottingen, 1966), pp. 307–320; E. O. Kane, Phys. Rev. 127, 131 (1962); Ref. 2.
[21]If many-electron relaxation effects are important, e.g., for core levels, the density of states measured will of course not be the solid's equilibrium density of states.
[22]L. V. Keldysh, Zh. Eksp. Teor. Fiz. 47, 1515 (1964) [Sov. Phys.-JETP 20, 1018 (1965)].
[23]Apart from the assumption, cf. Fig. 2(a), that the sample is finite in size.
[24]We use the gauge in which the scalar potential is everywhere zero.
[25]We neglect magnetic effects in all that follows. Thus we sum over electron-spin polarizations.
[26]Caroli *et al.*, Ref. 15, only look in detail at the case in which the light beam is incident normally on the surface, and make no serious attempt to incorporate lattice periodicity into their formulas properly.
[27]We measure energies from the vacuum level.
[28]We ignore the effects of the image force, which in any event is not present in the independent-particle picture of a solid. For a discussion of this latter point see, e.g., P. J. Feibelman, C. B. Duke, and A. Bagchi, Phys. Rev. B 5, 2436 (1972).
[29]Adawi (Ref. 16) only treats the simple model in which effects of the crystal lattice are ignored. However, there is no reason, in principle, why the validity of his Eq. (23b) is restricted to that model.
[30]Equation (16) is in some ways even more useful than Eq. (17). For example, in Eq. (16) the normalization of the occupied electron states is implicit. In Eq. (17) one must evaluate it.
[31]M. Gell-Mann and M. L. Goldberger, Phys. Rev. 91, 398 (1953); G. Breit and H. A. Bethe, Phys. Rev. 93, 888 (1954).
[32]The superscript r stands for "reduced zone scheme."
[33]That is, it satisfies an equation similar to Eq. (21).
[34]This subscript is absent for "surface bands."
[35]As well as in other photoabsorption calculations.
[36]D. Pines, *Elementary Excitations in Solids* (Benjamin, New York, 1964), p. 172. See also N. Wiser, Phys. Rev. 129, 62 (1963) and L. Hedin, A. Johansson, B. I. Lundquist, S. Lundquist and V. Samathiyakanit, Ark. Fys. 39, 97 (1969).
[37]K. Mitchell, Proc. R. Soc. Lond. A 146, 442 (1934); R. E. B. Makinson, Proc. R. Soc. Lond. A 162, 367 (1937); L. I. Schiff and L. H. Thomas, Phys. Rev. 47, 860 (1935).
[38]If U and V correspond to Schrödinger equations with the same Hamiltonian then the term $\vec{\epsilon}_{\parallel}\cdot\vec{k}_{\parallel}^{(r)}$ in Eq. (27) gives a vanishing contribution, by orthogonality. However if U corresponds to a solution of a Schrödinger equation in which the potential has an imaginary part, to represent inelastic scattering, while V corresponds to a real potential, then U and V cannot be expected to be orthogonal.
[39]If the light is totally reflected, then it is the electromagnetic energy density inside the sample, rather than the transmitted flux, which is relevant.
[40]Equivalent point is defined with respect to the bulk substrate lattice periodicity.
[41]"Evanescent" means falling to zero exponentially as $z\to\infty$. "Propagating" means behaving as a bulk Bloch wave as $z\to\infty$.
[42]At least a gap in the "projected" E-vs-$\vec{k}$ relation, i.e., projected by fixing $\vec{k}_{\parallel}^{(r)}$.
[43]Particularly, of course, when the electron escape depth is short.
[44]J. A. Appelbaum and D. R. Hamann, Phys. Rev. Lett. 32, 225 (1974); 31, 106 (1973).
[45]E. Caruthers, L. Kleinman, and G. P. Alldredge, Phys. Rev. B 8, 4570 (1973); 9, 3325 (1974); 9, 3330 (1974).
[46]D. Hamann and J. Appelbaum, Phys. Rev. B 6, 2166 (1972); G. P. Alldredge and L. Kleinman, Phys. Rev. B 10, 559 (1974).
[47]It is only true that the p_n's for Bloch waves incident onto the surface coincide with those for reflected Bloch waves, directed toward the crystal interior if the bulk crystal is sufficiently symmetric, and if the surface exposed is of sufficiently low Miller indices. That is, if we have a solution to the Schrödinger equation:

$$\left(E-\frac{(k_{\parallel}-G_{\parallel})^2+(p-G_{\perp})^2}{2m}\right)c_{G_{\parallel}G_{\perp}}=\sum_{G_{\parallel}'G_{\perp}'}V_{G_{\parallel}-G_{\parallel}',G_{\perp}-G_{\perp}'}\,c_{G_{\parallel}'G_{\perp}'},$$

it is not obvious that there will exist a solution to the reflected wave equation,

$$\left(E-\frac{(k_{\parallel}-G_{\parallel})^2-(p+G_{\perp})^2}{2m}\right)b_{G_{\parallel}G_{\perp}'}=\sum_{G_{\parallel}'G_{\perp}'}V_{G_{\parallel}-G_{\perp}',G_{\perp}-G_{\perp}'}\,b_{G_{\parallel}'G_{\perp}'}.$$

We can only be sure of finding such a solution if (a) $V_{G_{\parallel}G_{\perp}}=V_{G_{\parallel}-G_{\perp}}$ or if (b) $V_{G_{\parallel},G_{\perp}}=V_{-G_{\parallel},G_{\perp}}$. In the first instance, $b_{G_{\parallel}G_{\perp}}=c_{G_{\parallel},-G_{\perp}}$, while in the second we find that $b_{G_{\parallel},G_{\perp}}=c^{*}_{G_{\parallel},-G_{\perp}}$. In the present paper we assume for simplicity that either (a) or (b) is satisfied.
[48]That is, ordinary lattice periodicity for values of $z>0$ and two-dimensional lattice periodicity for all z.
[49]Hole damping can be treated within the present formalism. A qualitative discussion is given in Sec. IV.
[50]We are in the reduced-zone scheme, here.
[51]See also Ref. 6, Sec. 5. A similar discussion was given there for the case of the nearly-free-electron solid.
[52]This theorem may easily be proven, cf., e.g., R. More, Phys. Rev. B (to be published). The theorem implies that the fact that we chose to define our occupied states, in Eq. (38), as having a single Bloch wave incident on the surface plus reflected waves, rather than, e.g., a single reflected wave and many incident ones

makes no difference in our final result, Eq. (49).

[53]We have neglected the attenuation of the electromagnetic wave due to its absorption in photoexcitation processes. Had we included this effect, via the multiplication of $\vec{A}$ by a factor $e^{-\alpha z}$, then $[k_{\perp}^{(2)}(n'')]^{-1}$ would be replaced by $[k_{\perp}^{(2)}(n'')+\alpha]^{-1}$. In general, $\alpha^{-1} \gtrsim 10^2$ Å while $(k_{\perp}^{(2)})^{-1} \approx 5 \sim 30$ Å, which justifies our neglect of α.

[54]R. More, Phys. Rev. B (to be published).

[55]$\Theta(x)$ is the ordinary step function.

[56]Note that we can now extend the sum on n'' formally to include values for which Bloch states exist inside the crystal, having $P(n'', k_{\parallel}^{(r)} \cdots) = 0$. Thus the sum of n'' can now be said to include all n''.

[57]E. O. Kane, Phys. Rev. 175, 1039 (1968).

[58]W. D. Grobman and D. E. Eastman, Surf. Sci. 37, 355 (1973).

[59]J. C. Tracy, J. Vac. Sci. Technol. 11, 280 (1974).

[60]C. J. Powell, Surf. Sci. 44, 29 (1974).

[61]Apart from relaxation effects and transition-probability weighting factors.

[62]D. E. Eastman (unpublished).

[63]D. E. Eastman and M. Kunznietz, J. Appl. Phys. 42, 1396 (1971).

[64]E. O. Kane, J. Phys. Soc. Jpn. Suppl. 21, 37 (1966).

[65]J. F. Janak, D. E. Eastman, and A. R. Williams, *Electronic Density of States Symposium*, 1969 (Natl. Bur. Std. Spec. Publ. No. 323 (U. S. GPO, Washington, D. C., 1971), p. 181.

[66]E. Kane, Phys. Rev. 159, 624 (1967).

[67]J. E. Demuth and D. E. Eastman, Phys. Rev. Lett. (to be published).

[68]D. A. Shirley, Chem. Phys. Lett. 16, 220 (1972).

[69]H. D. Hagstrum and G. E. Becker, Phys. Rev. B 8, 107 (1973).

[70]P. H. Citrin and D. R. Hamann, Chem. Phys. Lett. 22, 301 (1973).

[71]G. K. Wertheim and S. Hufner, Phys. Rev. Lett 28, 1028 (1972).

[72]P. A. Cox, Y. Baer, and C. K. Jorgensen, Chem. Phys. Lett. 22, 433 (1973).

[73]D. E. Eastman, F. Holtzberg, J. Freeouf, and M. Erbudak, AIP Conf. Proc. 18, 1030 (1974).